Received November 25, 2020, accepted December 7, 2020, date of publication December 14, 2020,
date of current version January 4, 2021.

Digital Object Identifier 10.1109/ACCESS.2020.3044546

Polar-Coded OFDM With Index Modulation

**SI-YU ZHANG, (Graduate Student Member, IEEE),
AND BEHNAM SHAHRRAVA, (Member, IEEE)**
Department of Electrical and Computer Engineering, University of Windsor, Windsor, ON N9C 3P4, Canada
Corresponding author: Si-Yu Zhang (zhang1fs@uwindsor.ca)

ABSTRACT In this paper, we apply polar codes to a modified version of OFDM systems with index modulation which is called OFDM with in-phase/quadrature index modulation (OFDM-I/Q-IM). We provide general design guidelines for the proposed polar-coded OFDM-I/Q-IM systems. In the proposed system, at the transmitter, we employ a random frozen bits appending scheme which not only makes the polar code compatible with OFDM-I/Q-IM but also improves the bit error rate (BER) performance of the system. Furthermore, at the receiver, it is shown that the *a posteriori* information for each index provided by the index detector is essential for the iterative decoding of polar codes by the belief propagation (BP) algorithm. Simulation results show that the proposed polar-coded OFDM-I/Q-IM system outperforms its OFDM counterpart in terms of BER performance.

INDEX TERMS Bit error rate (BER), orthogonal frequency division multiplexing (OFDM), index modulation, polar codes, log-likelihood ratio (LLR).

I. INTRODUCTION

Polar codes, introduced by Arikan in 2009 [1], can achieve symmetric capacity of binary-input discrete memoryless channels (B-DMC) for the input letters with equal probability. In some scenarios, it has been shown that the bit-error-rate (BER) performance of polar codes can be similar to that of turbo or LDPC codes with lower complexity by utilizing successive cancellation list (SCL) decoding scheme [2]. Furthermore, the polar codes aided by cyclic redundancy check (CRC) can achieve even better performance than other channel coding schemes [3]. For these reasons, polar coding has been adopted to the 5G new radio (NR) interface by the third-generation partnership project (3GPP) [4].

Beside applying polar coding, to meet the requirements of the next generation of high-speed wireless communication networks, also new waveform formats have been proposed. The orthogonal frequency division multiplexing with index modulation (OFDM-IM) is a modified version of OFDM by extending the concept of spatial modulation (SM) to the frequency domain. The idea of OFDM-IM was firstly proposed in [5], and an overview of this technique can be found in [6], [7]. Compared with the conventional OFDM, OFDM-IM offers a trade-off between energy efficiency and system performance with the adjustment of the number of active sub-carriers in the system [8]. Hence, OFDM-IM is suitable for some businesses in next generation communication networks. Since OFDM-IM has unique advantages, as an extended version of OFDM, it is also considered as a promising candidate for 5G [9]. However, OFDM-IM performs weaker than OFDM in low signal-to-noise ratio (SNR) [5]. Hence, some modified OFDM-IM schemes with better performance have been proposed. In [10], the number of active sub-carriers was adaptive, which increased the spectral efficiency (SE) of OFDM-IM. In [11], interleavers were adopted to enhance the performance of OFDM-IM at the cost of higher latency. In [8] and [12], two methods with higher diversity gain were introduced, which significantly improved the performance of OFDM-IM while reducing SE. In [13], OFDM in-phase/quadrature IM (OFDM-I/Q-IM), which can be considered as a generalized OFDM-IM, was proposed. Compared with the conventional technique, OFDM-I/Q-IM not only has higher SE but also achieves better BER performance. Hence, OFDM-I/Q-IM can be considered as a promising candidate for the next generation of high-speed wireless communication networks.

The application of polar codes in conventional OFDM systems has been discussed in [14]. It has been shown the design of a polar-coded OFDM system is very straight forward. However, a major drawback of polar-coded OFDM systems is that increasing the transmission rate in these systems leads to substantial performance degradation [15]. Because of some advantages of OFDM with index modulation, it seems intuitively that polar-coded OFDM-IM or polar-coded OFDM-I/Q-IM systems can outperform their OFDM counterpart. However, combining polar codes with

The associate editor coordinating the review of this manuscript and approving it for publication was Xueqin Jiang.

any type of OFDM-IM is a challenging problem, whereas the design of polar-coded OFDM is very straightforward. It is shown that the idea of applying polar codes in the conventional OFDM-IM scheme [5], [16]–[18] is limited to the case in which a BPSK modulator is employed as a symbol mapper; while, in practice, the design of most systems is based on higher order modulations to reach higher spectral efficiency. Hence, in this paper, we focus on OFDM-I/Q-IM since it has more flexibility in the allocation of bits in a polar-coded system and also better performance compared to OFDM-IM. We try to provide a general design guideline for polar-coded OFDM-I/Q-IM.

Application of polar codes in OFDM-I/Q-IM systems presents new challenges, and dealing with these is the main focus of this paper. One of the challenges is to combine polar coding with restricted length with OFDM-I/Q-IM modulators employing different constellations symbols. The other challenge is to include the *a posteriori* information provided by the index detector for polar decoding to take further advantage of the structure signaling. Hence, in order to propose a polar-coded OFDM-IM system, the following step will be taken:

- In the proposed system, at the transmitter, in order to make the polar code compatible with OFDM-I/Q-IM, we employ a random frozen bits appending scheme. In the design of polar-coded OFDM-I/Q-IM, this novel scheme not only helps us to make the polar code compatible with OFDM-I/Q-IM but also improves the BER performance of the system.
- At the receiver, the channel detectors, based on the received signal and the a priori information, provide soft information for both the index detector and the polar decoder. Next, the index detector produces the *a posteriori* information for the index bits, by utilizing the information from the channel detectors and the lookup tables for mapping. Then, the information provided by the index detector is fed to the polar decoder. Finally, the proposed polar decoder, which is based on the belief propagation (BP) algorithm, computes the *a posteriori* information for the information bits based on the code constraints, the input information given by the channel detectors and utilizing the information provided by the index detector.

The remainer of this paper is organized as follows. Section II gives the preliminary knowledge, including polar codes and OFDM-I/Q-IM. We give the proposed polar-coded OFDM-I/Q-IM system in section III by introducing its transmitter and receiver, respectively. Simulation results of the proposed system are presented and evaluated in section IV. The conclusion of this paper is given in section V.

II. PRELIMINARY KNOWLEDGE

In this section, a background knowledge of polar codes is presented first. Then, the OFDM-I/Q-IM technique is introduced.

A. POLAR CODES

Polar codes can achieve channel capacity through channel polarization [1], which operates N synthetic channels from N independent channels of a B-DMC. The polarized channels with near one capacity are regarded as noiseless, and selected to carry information bits. The rest unreliable channels are set to fix-valued bits. These bits are called frozen bits. We note that the values and positions of frozen bits are pre-known by transceivers. An important thing for polar codes construction is to determine the noiseless channels. Bhattacharyya parameters [1] and Gaussian approximation (GA) [19] are common ways to build a polar code. We note that there are some works investigate polar codes design in channels with memory [20], [21]. For simplicity, in this paper, we apply GA scheme as the polar encoding method.

Let assume m information bits after $N-m$ zeros insertion, which are denoted as: $U_1^N = [U_1, U_2, \ldots, U_N]$, where N is the code length, m bits of U_1^N are messages, and the rest of them are frozen bits. The values and positions of frozen bits are known in advance by transceivers. The encoding process can be described as $X_1^N = U_1^N \mathrm{G}_2^{\otimes v}$, where $\mathrm{G}_2 = \begin{bmatrix} 1 & 0 \\ 1 & 1 \end{bmatrix}$, $v = \log_2 N$, and $\mathrm{G}_2^{\otimes v}$ indicates the v^{th} Kronecker product of G_2. The code rate R_{code} is defined as: m/N.

B. OFDM WITH IN-Phase/QUADRATURE INDEX MODULATION

By independently implementing index modulation on the in-phase and quadrature components of OFDM signals, OFDM-I/Q-IM achieves more transmit diversity than conventional OFDM-IM. Moreover, thanks to the higher SE, OFDM-I/Q-IM is able to transmit polar-coded signals, which may have restricted length and variant constellations. Hence, in this paper, we apply OFDM-I/Q-IM to the proposed system to achieve better performance and flexibility. This sub-section gives a brief introduction on OFDM-I/Q-IM.

The block diagram of an OFDM-I/Q-IM transmitter is given in Fig.1.(a). For OFDM-I/Q-IM, the available number of sub-carriers is denoted as: N_{fft}. First, m information bits U_1^m are divided into $2G$ groups, each of which has p bits, thus $m = 2Gp$. Each group of p bits are sent to an OFDM-I/Q-IM modulator to generate an in-phase or quadrature component of an OFDM sub-block with n available sub-carriers, where $n = N_{fft}/G$. Unlike conventional OFDM-IM that maps a complex symbol to an available sub-carrier, OFDM-I/Q-IM implements index modulation on in-phase and quadrature dimensions separately. The p bits of an OFDM-I/Q-IM sub-block are divided into two parts: the first p_1 bits are used for index modulation, and the remaining p_2 bits are mapped to constellations on in-phase or quadrature dimension. Let take the first p bits on in-phase dimension as an example, the p_1 bits $\mathbf{i}_1^I = [i_1^I(1), \ldots, i_1^I(p_1)]$, where $i_1^I(\alpha) \in \{0, 1\}$, are sent to an index selector to generate an indices indicator $\mathbf{I}_1^I$, which indicates to activate k sub-carriers out of n available ones, while the rest of $n-k$ sub-carriers are null. For the g^{th}

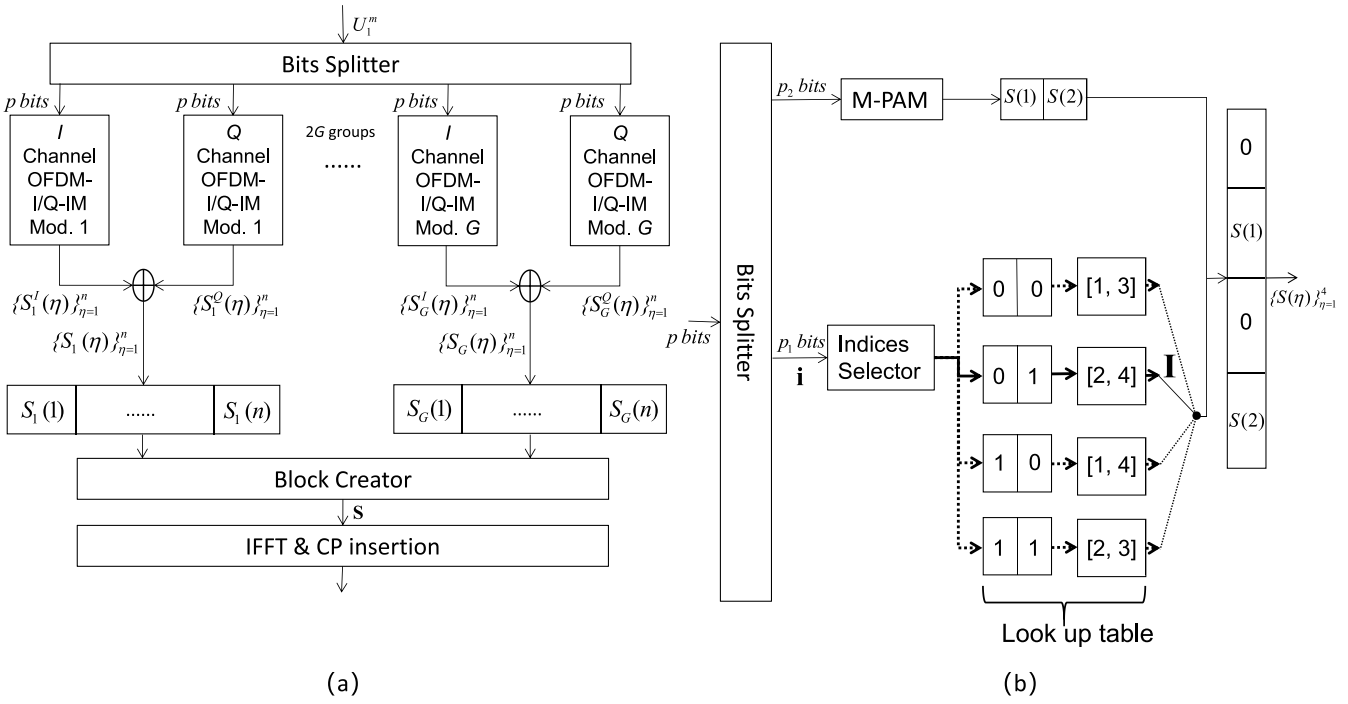

FIGURE 1. System model of (a).an OFDM-I/Q-IM transmitter (b). an example of an OFDM-I/Q-IM modulator for $n = 4$, $k = 2$.

$(1 \le g \le G)$ sub-block, the indices of k active sub-carriers in the in-phase and quadrature dimensions are denoted as:

$$\mathbf{I}_g^I = [I_g^I(1), \ldots, I_g^I(k)],\ \mathbf{I}_g^Q = [I_g^Q(1), \ldots, I_g^Q(k)] \quad (1)$$

where $I_g^I(\gamma), I_g^Q(\gamma) \in \{1, \ldots, n\}$ for $\gamma = 1, \ldots, k$. The indices selection is implemented by using the look-up table or combinational methods [5]. Then, based on the first p_1 bits of $\mathbf{i}_g$, the remaining p_2 bits are mapped to M-PAM symbols in in-phase/quadrature dimensions. After index modulation using the first p_1 bits, the in-phase/quadrature part of the g^{th} OFDM sub-block can be denoted as:

$$\mathbf{S}_g^I = \begin{cases} S_g^I(\eta), & \eta \in \mathbf{I}_g^I \\ 0, & \text{otherwise,} \end{cases} \quad \mathbf{S}_g^Q = \begin{cases} S_g^Q(\eta), & \eta \in \mathbf{I}_g^Q \\ 0, & \text{otherwise} \end{cases} \quad (2)$$

where $S_g^I(\eta)$ and $S_g^Q(\eta)$ are independently obtained from a M-PAM constellation Θ for $\eta = 1, \ldots, n$. Then, the in-phase/quadrature parts in (2) are combined to generate a complex OFDM sub-block:

$$\mathbf{S}_g = \mathbf{S}_g^I + j\mathbf{S}_g^Q, \quad g = 1, 2, \ldots G. \quad (3)$$

An OFDM-I/Q-IM encoder with $n = 4$, $k = 2$ using Table.1 is given in Fig.1.(b). In this example, if the first p_1 bits is [0, 1], then the symbols $S(1)$ and $S(2)$ generated by the p_2 bits should occupy the 2^{nd} and 4^{th} sub-carriers while the rest ones are idle.

After concatenating $\mathbf{S}_g$, the OFDM block is transformed to time domain by using N_{fft} points inverse fast Fourier transform (IFFT). After P/S converter and cyclic prefix (CP) insertion. The vector is sent to a frequency selective channel. The transmission rate of the OFDM-I/Q-IM is:

TABLE 1. A look-up table example for $k = 2$, $n = 4$, $p_1 = 2$.

Pattern	Bits $\mathbf{i}$	Indices $\mathbf{I}$
P_1	[0, 0]	[1, 3]
P_2	[0, 1]	[2, 4]
P_3	[1, 0]	[1, 4]
P_4	[1, 1]	[2, 3]

$$R = \frac{2(p_1 + p_2)}{n} = 2G\left(\frac{\lfloor \log_2 \mathbb{C}_n^k \rfloor + k \log_2 M}{N_{fft}}\right) \quad (4)$$

where $\lfloor\ \rfloor$ is the floor function and $\mathbb{C}$ is the combinatorial operation.

At the receiver, after the removal of CP, a FFT operation needs to be implemented. The OFDM-I/Q-IM receiver needs to detect both the indices of active sub-carriers and the corresponding data symbols. For each sub-block, by considering a joint detection for the indices of active sub-carriers and the transmitted symbols carried on, the maximum likelihood (ML) detector for OFDM-I/Q-IM is given by [13]:

$$\{\hat{S}_g(\eta)\}_{\eta=1}^n = \underset{\{S_g(\eta)\}_{\eta=1}^n}{\operatorname{argmin}} \sum_{\eta=1}^{n} |y_g(\eta) - H_g(\eta) S_g(\eta)|^2 \quad (5)$$

where $H_g(\eta)$ denotes the channel frequency response (CFR) on the η^{th} sub-carrier of the g^{th} sub-block. More details for ML decoding in OFDM-I/Q-IM can be found in [13]. The searching space of the ML detection per bit is given by the order of $O(\binom{n}{k} + M^k)$ [22]. Hence the optimal ML detector has high complexity. To achieve near optimal performance, two low-complex detectors have been proposed, including the low-complex ML and the *a posteriori* probability detection

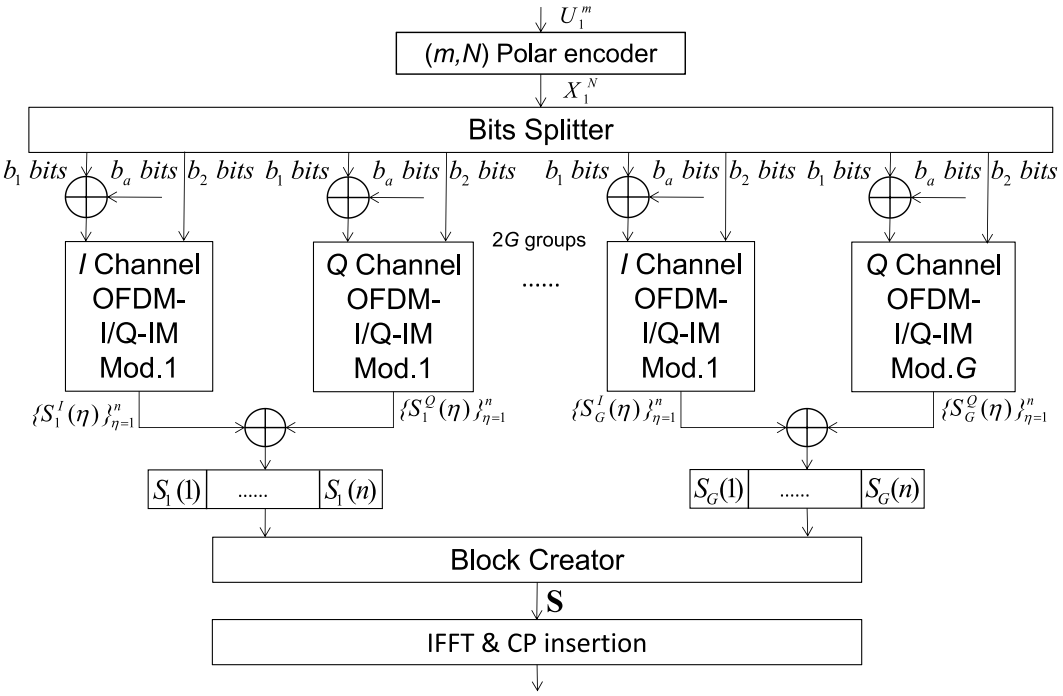

FIGURE 2. Block diagram of the proposed polar-coded OFDM-I/Q-IM transmitter.

methods [9]. In this paper, the *a posteriori* probability detection method is used and the corresponding process will be introduced in the next section. The OFDM-I/Q-IM can obtain around 4-6 dB performance gains in mid-high SNR compared with the conventional OFDM scheme [13].

III. THE PROPOSED POLAR CODED OFDM-I/Q-IM SYSTEM

The powerful polar codes allow us to achieve channel capacity performance. In this section, the polar-coded OFDM-I/Q-IM is proposed, and the design guideline of the system is introduced in terms of the transmitter and receiver, respectively.

A. THE TRANSMITTER DESIGN

Block diagram of the proposed polar-coded OFDM-I/Q-IM transmitter is given in Fig.2. The system aims to transmit m-bits message U_1^m. These bits are processed by a polar encoder to have a length N codeword X_1^N. Then, they are divided into $2G$ groups, each of which contains b bits. These b bits need to be further divided into two parts, which contain b_1 and b_2 bits for index modulation and constellation mapping, respectively.

We note that the amount of bits carried by a pure OFDM-I/Q-IM must be $2G(k\log_2 M + \lfloor \log_2 \mathbb{C}_n^k \rfloor)$, which is not always equal to the length of a polar code (We note that although in some works, polar codes can be constructed with variant length [23], [24], these methods suffered performance degradation.). Therefore, compared with a pure OFDM-I/Q-IM, when applying polar coding, the selection of b_1 and b_2 have to be carefully implemented when splitting bits. For a polar-coded OFDM-I/Q-IM, the available b_1 and b_2 needs to be selected based on the following rule:

$$G(b_1 + b_2) \geq k\log_2^M + \lfloor \log_2 \mathbb{C}_n^k \rfloor \tag{6}$$

Proof: first, we assume the length of a polar code is 2^v, thus $G(b_1 + b_2) = 2^{v-1}$. Then, since each b_2 bits need to be modulated by M-PAM, we have $\frac{2^{v-1}}{G} - b_1 = k\log_2 M$. Moreover, the first group of b_1 bits are required for index modulation. In a pure OFDM-I/Q-IM system, b_1 is required to be exactly equal to $\lfloor \log_2 \mathbb{C}_n^k \rfloor$. Nevertheless, as long as $b_1 \leq \lfloor \log_2 \mathbb{C}_n^k \rfloor$, the b_2 bits can be successfully used for index modulation. Therefore, we use this loose constraint in the proposed polar-coded OFDM-I/Q-IM. Combining the above three conditions, we can obtain (6). For an example, considering a length $N = 128$, $N_{fft} = 64$, and 4-QAM polar-coded OFDM-I/Q-IM system. If $G = 16$, we can set $b_1 = b_2 = 2$ bits, $n = 4$, and $k = 2$. In such scenario, the value b_1 for index modulation is exactly equivalent to p_1 that is used in pure OFDM-I/Q-IM systems, and Table.1 can be used. However, considering a pure OFDM-I/Q-IM case with $G = 8$, thus $n = 8$, if we set $k = 6$, the corresponding p_1 should be 4 bits. However, since the length of polar code is $N = 128$, for a 4-QAM system, the amount of available bits for index modulation is only 32, thus b_1 has to be 2 bits, resulting in $b_1 < p_1$. To activate 6 out of 8 available sub-carriers with less bits, instead of all 16 patterns, only 4 sub-carrier activation patterns (SAPs) can be selected, which is shown in Table.2. However, to maintain the compatibility of OFDM-I/Q-IM with polar codes, in this paper, we propose a scheme that appends $b_a = p_1 - b_1$ random frozen bits $\mathbf{U}_f$ at the end of the original b_1 length index vector. We take a 2-bit-length vector $\mathbf{i}^I = [i^I(1), i^I(2)]$ in the in-phase dimension as an example.

TABLE 2. A look-up table example for $k = 6$, $n = 8$, $b_1 = 2$.

Pattern	Bits $\mathbf{i}$	Indices $\mathbf{I}$
P_1	[0, 0]	[2, 4, 5, 6, 7, 8]
P_2	[0, 1]	[1, 3, 5, 6, 7, 8]
P_3	[1, 0]	[1, 2, 3, 4, 6, 8]
P_4	[1, 1]	[1, 2, 3, 4, 5, 7]

TABLE 3. A look-up table example for $k = 6$, $n = 8$, $b_1 = 2$, $b_a = 2$.

Pattern	Bits $[i(1), i(2), U_f(\zeta), U_f(\zeta+1)]$	Indices $\mathbf{I}$
P_1	[0, 0, 0, 0]	[2, 4, 5, 6, 7, 8]
P_2	[0, 0, 0, 1]	[2, 3, 5, 6, 7, 8]
P_3	[0, 0, 1, 0]	[2, 3, 4, 6, 7, 8]
P_4	[0, 0, 1, 1]	[2, 3, 4, 5, 7, 8]
P_5	[0, 1, 0, 0]	[1, 3, 5, 6, 7, 8]
P_6	[0, 1, 0, 1]	[1, 2, 5, 6, 7, 8]
P_7	[0, 1, 1, 0]	[1, 2, 3, 6, 7, 8]
P_8	[0, 1, 1, 1]	[1, 2, 3, 5, 7, 8]
P_9	[1, 0, 0, 0]	[1, 2, 3, 4, 6, 8]
P_{10}	[1, 0, 0, 1]	[1, 2, 3, 5, 6, 8]
P_{11}	[1, 0, 1, 0]	[1, 2, 3, 4, 5, 8]
P_{12}	[1, 0, 1, 1]	[1, 2, 3, 4, 5, 6]
P_{13}	[1, 1, 0, 0]	[1, 2, 3, 4, 5, 7]
P_{14}	[1, 1, 0, 1]	[1, 2, 3, 4, 7, 8]
P_{15}	[1, 1, 1, 0]	[1, 3, 4, 5, 6, 7]
P_{16}	[1, 1, 1, 1]	[1, 4, 5, 6, 7, 8]

To align with the pure OFDM-I/Q-IM that requires 4 bits for IM, two frozen bits needs to be appended at the end of $\mathbf{i}^I$, given by:

$$\mathbf{i}^I = [i^I(1), i^I(2), U_f(\zeta), U_f(\zeta+1)] \tag{7}$$

where $U_f(\zeta) \in \{0, 1\}$ is the ζ^{th} frozen bit, and $1 \leq \zeta \leq N - m$. Therefore, similar to the pure OFDM-I/Q-IM, all $2^4 = 16$ SAPs in Table.3 have a chance to be selected. At the receiver, since $U_f(\zeta)$, $U_f(\zeta+1)$ are pre-known, the selector only needs to choose patterns that the last two bits are $U_f(\zeta)$ and $U_f(\zeta+1)$ as possible answers. For example, based on Table.3 and pre-known frozen bits (for example: $U_f(\zeta) = 0$, $U_f(\zeta+1) = 0$), the estimated SAP can be only selected from P_1, P_5, P_9, P_{13}.

By using the random frozen bits, the available SAPs are extended. This proposed method is equivalent to a random interleaver, which may provide potential benefit to the proposed system. Here, we briefly analyze the advantage of the appending method using random $\mathbf{U}_f$ compared with the scheme that uses fixed frozen bits (The conventional scheme without appending frozen bits is equivalent to that uses fixed bits.) based on distance. First, we introduce the following definitions. For a n-elements vector $\mathbf{V}_g = [V_{g,1}, V_{g,2}, \ldots, V_{g,n}]$, the distance between any two vectors $\mathbf{V}_m$ and $\mathbf{V}_q$ is given as: $D(m, q) = \sqrt{\sum_{j=1}^{n} |V_{m,j} - V_{q,j}|^2}$. For simplicity, we consider an all one BPSK OFDM-I/Q-IM system with $n = 4$, $k = 2$, and $p_1 = 1$. We assume that sub-carriers in the same sub-block have similar CFR H_g. In this case, based on Table.1, the average distance (AD) of the appending method using fixed frozen bits (0) in a single OFDM block is derived as:

$$AD_f = \frac{2\sqrt{2}}{G(G-1)} \sum_{g=1}^{G-1} \sum_{i=g+1}^{G} |H_g - H_i| \tag{8}$$

Then, using the same system above, we assume that the first sub-block utilizes a non-zero appending frozen bit, such as 1. Based on Table.1, the AD of the appending method using random frozen bits in a single OFDM block is derived as:

$$AD_r = \frac{2\sqrt{2}}{G(G-1)} \left(\sum_{g=2}^{G} \sqrt{|H_1|^2 - |H_g|^2} + \sum_{g=2}^{G-1} \sum_{i=g+1}^{G} |H_g - H_i|\right) \tag{9}$$

The difference between AD_r and AD_f, denoted by Δ, is expressed as

$$\begin{aligned} \Delta &= AD_r - AD_f \\ &= \frac{2\sqrt{2}}{G(G-1)} \sum_{g=2}^{G} \left(\sqrt{|H_1|^2 + |H_g|^2} - |H_1 - H_g|\right) \end{aligned} \tag{10}$$

The advantage of the proposed appending method using random frozen bits over the one using fixed frozen bits Δ is proved in the case of $\Delta \geq 0$, i.e.

$$\left(\sqrt{|H_1|^2 + |H_g|^2} - |H_1 - H_g|\right) \geq 0 \tag{11}$$

The inequality (11) can be shown to hold as follows:

$$\begin{aligned} &\left(\sqrt{|H_1|^2 + |H_g|^2} - |H_1 - H_g|\right) \geq 0 \\ &\Rightarrow (|H_1|^2 + |H_g|^2) - |H_1 - H_g|^2 \geq 0 \\ &\Rightarrow 2|H_1||H_g| \geq 0 \end{aligned} \tag{12}$$

Simulation results in the following section also verified above assumption that compared with the appending method using fixed frozen bits, the proposed appending method is helpful to decrease the BER.

The bits after appending $\mathbf{U}_f$ can be treated by an OFDM-I/Q-IM modulator given in Fig.1.(b). Then, after IFFT and CP insertion, an OFDM block is generated and transmitted. Also, as what we note before, an advantage of OFDM-I/Q-IM compared with OFDM-IM is that OFDM-I/Q-IM is more flexible for polar-coded systems when variant constellations are applied. After introducing the bits appending method, we show the advantage of OFDM-I/Q-IM for polar-coded systems in Table.4, where b_a is the number of random frozen bits appended after the original b_1 bits. Table.4 illustrates that with the restriction of polar codes, OFDM-I/Q-IM can be adopted in more scenarios, which is more flexible than OFDM-IM. For the proposed system, unlike pure OFDM-I/Q-IM, b_1, b_2, b_a need to be carefully selected under the restriction of polar codes.

B. THE RECEIVER DESIGN

After removing CP and invoking the fast Fourier transform (FFT), unlike the conventional polar-coded OFDM system, the proposed polar-coded OFDM-I/Q-IM system needs to detect the indices of active sub-carriers and the corresponding information bits according to the received vector $y(\beta)$ with $\beta = 1, 2, \ldots, N_{fft}$. In this paper, the channel detector in [5] is applied to obtain the active indices patterns $\mathbf{I}_g^I$ and $\mathbf{I}_g^Q$. We note that the indices detection for the in-phase and quadrature parts

TABLE 4. The bits allocation schemes for polar-coded OFDM-IM and polar-coded OFDM-I/Q-IM with $N_{fft} = 128$.

	Const.	k	n	b_1	b_2	b_a
Polar-OFDM-IM	BPSK	2	4	2	2	0
		5	8	3	5	2
	4-QAM	2	4	Not Available		
		5	8	Not Available		
	16QAM	2	4	Not Available		
		5	8	Not Available		
		6	8	Not Available		
Polar-OFDM-I/Q-IM	BPSK	2	4	2	2	0
		5	8	5	5	2
	4-QAM	2	4	2	2	0
		5	8	5	5	2
	16-QAM	2	4	Not Available		
		5	8	Not Available		
		6	8	4	12	0

are same and implemented simultaneously. Hence, in the following section, we only take the in-phase sub-blocks as an example, and the superscript I is omitted for simplicity.

The channel detector of OFDM-I/Q-IM gives the *a posteriori* probabilities of frequency domain signals by considering the case that the values are either non-zero or zero [5]. For the g^{th} sub-block, channel detectors provide the probability of the active status of the corresponding index η with $\eta = 1, 2, \ldots, n$, given by:

$$\lambda_g(\eta) = \ln \frac{\sum_{\chi=1}^{M} P(S_g(\eta) = Q_\chi | y_g(\eta))}{P(S_g(\eta) = 0 | y_g(\eta))} \tag{13}$$

where Q_χ is the element of a M-array PAM constellation, and $y_g(\eta)$ is the received vector for the g^{th} sub-block after FFT operation, which can be written as:

$$y_g(\eta) = H_g(\eta) S_g(\eta) + w_g(\eta), \text{ for } \eta = 1, \ldots, n \tag{14}$$

where $w_g(\eta)$ denotes the zero-mean complex additive white Gaussian noise (AWGN) with variance σ_k^2 on the η^{th} sub-carrier of the g^{th} sub-block. It is assumed that the noise variance in the time domain is σ^2, which is related with the noise variance in the frequency domain via $\sigma_k^2 = (k/n)\sigma^2$ due to the normalization factor $\sqrt{(k/n)}$ of the FFT at the receiver [10].

The lager the value of $\lambda(\eta)$, the higher the probability that the corresponding η is an active sub-carrier. Using Bayes formula, (13) can be expressed as:

$$\lambda(\eta) = \ln(k) - \ln(n-k) + \frac{|y_g(\eta)|^2}{\sigma_k^2} + \ln\Big(\sum_{\chi=1}^{M} \exp\Big(-\frac{1}{\sigma_k^2} |y_g(\eta) - H_g(\eta) Q_\chi|^2\Big)\Big) \tag{15}$$

The complexity of a channel detector is $O(M)$ per sub-carrier and dimension. Also, like conventional OFDM-IM, the Jacobian logarithm [25] can be applied in (15). For example, the identity $\ln(e^{a_1} + e^{a_2}, \ldots + e^{a_M}) = \int_{max}(\int_{max}(\int_{max}(a_1, a_2), a_3, \ldots), a_M)$, where $\int_{max}(a, b) = \ln(e^{a_1} + e^{a_2}) = \max(a_1, a_2) + \ln(1 + e^{-|a_1 - a_2|})$ can be utilized to simplify (15). Then, the channel detector can do conjunction based on a look-up table. Let denote the set of possible active indices of the g^{th} sub-block by $\mathbb{I} = \{\mathbf{I}_g^1, \mathbf{I}_g^2, \ldots, \mathbf{I}_g^V\}$ for which $\mathbf{I}_g^\omega \in \mathbb{I}$, where $\mathbf{I}_g^\omega = [I_g^\omega(1), I_g^\omega(2), \ldots, I_g^\omega(k)]$ with $\omega = 1, .., V$ and $V = \lfloor \log_2 \mathbb{C}_n^k \rfloor$. For example, for Table.1, we have $\mathbf{I}_g^1 = [1, 3]$, $\mathbf{I}_g^2 = [2, 4]$, $\mathbf{I}_g^3 = [1, 4]$, $\mathbf{I}_g^4 = [2, 3]$. After obtaining all *a posteriori* probabilities based on (15), for each sub-block, the receiver can calculate the following V summations for all possible set of active indices using the corresponding look-up table as [5]:

$$d_g^\omega = \sum_{\gamma=1}^{k} \lambda(n(g-1) + I_g^\omega(\gamma)) \tag{16}$$

for $\omega = 1, 2, \ldots, V$. Let take Table.1 as an example, for sub-block g, we have $d_g^1 = \lambda(1) + \lambda(3)$, $d_g^2 = \lambda(2) + \lambda(4)$, $d_g^3 = \lambda(1) + \lambda(4)$, $d_g^4 = \lambda(2) + \lambda(3)$. Then, the receiver makes decision on the set of active sub-carriers based on the maximum sum among all V probability sums: $\hat{\omega} = \underset{\omega}{\text{argmax}} d_g^\omega$. Then, the estimated $\mathbf{I}_g$ can be mapped to the index bits $\mathbf{i}_g$ according to the corresponding look-up tables.

The block diagram of the proposed polar-coded OFDM-I/Q-IM receiver is given in Fig.3.(a). For each in-phase or quadrature sub-block g, after obtaining the estimated $\mathbf{I}_g$ from channel detectors, the initial LLRs for polar decoding need to be calculated. The initial LLRs of the index bits for decoding rely on the *a posteriori* information provided by the index detector, and the corresponding information can be calculated from the hard valued detected index bits or the soft information obtained from the *a posteriori* probabilities $\lambda(\eta)$ of channel detectors and look-up tables. These initial LLRs for polar decoding are more reliable than the LLRs used in polar-coded OFDM because the index error rate (IER) for OFDM-I/Q-IM is lower than the BER of M-QAM demodulation. The corresponding proof is given in appendix. Therefore, by utilizing these reliable initial LLRs, we expect that the proposed system can achieve better performance than that of polar-coded OFDM.

For each in-phase or quadrature sub-block g, after obtaining the estimated $\mathbf{I}_g$, these index indicators are de-mapped to the indices bits $\mathbf{i}_g = [X_g(1), X_g(2), \ldots, X_g(k)]$ based on look-up tables. After de-mapping all $\mathbf{i}_g$, the detected indices are combined to have a $2Gb_1$ length sequence $\mathbf{X}_{id}$. The initial LLRs for polar decoding can be obtained through $\mathbf{X}_{id}$, denoted as:

$$\mathbf{X}_{id} = [X_{id}(1), X_{id}(2) \ldots, X_{id}(2Gp_1)] \tag{17}$$

The LLRs obtaining method using hard information is given in the lower part of Fig.3.(b), where $\sqrt{E_b}$ is the energy per bit. This sequence (17) can be seen as a bit stream that is perfectly transmitted without affected by noise.

Nevertheless, intuitively, for a sub-block g with index bits $\mathbf{i}_g = [i(1), i(2), \ldots, i(b_1)]$, the initial LLR of index bit $i(j)$ in $\mathbf{i}_g$ can be obtained by fully utilizing the probability related to $\lambda(\eta)$. However, (15) only reflects the probability that the corresponding position η is zero or not. Therefore, by combining the look-up tables for mapping, we can indirectly obtain the LLR of $i(j)$ for polar decoding, where $1 \leq j \leq b_1$.

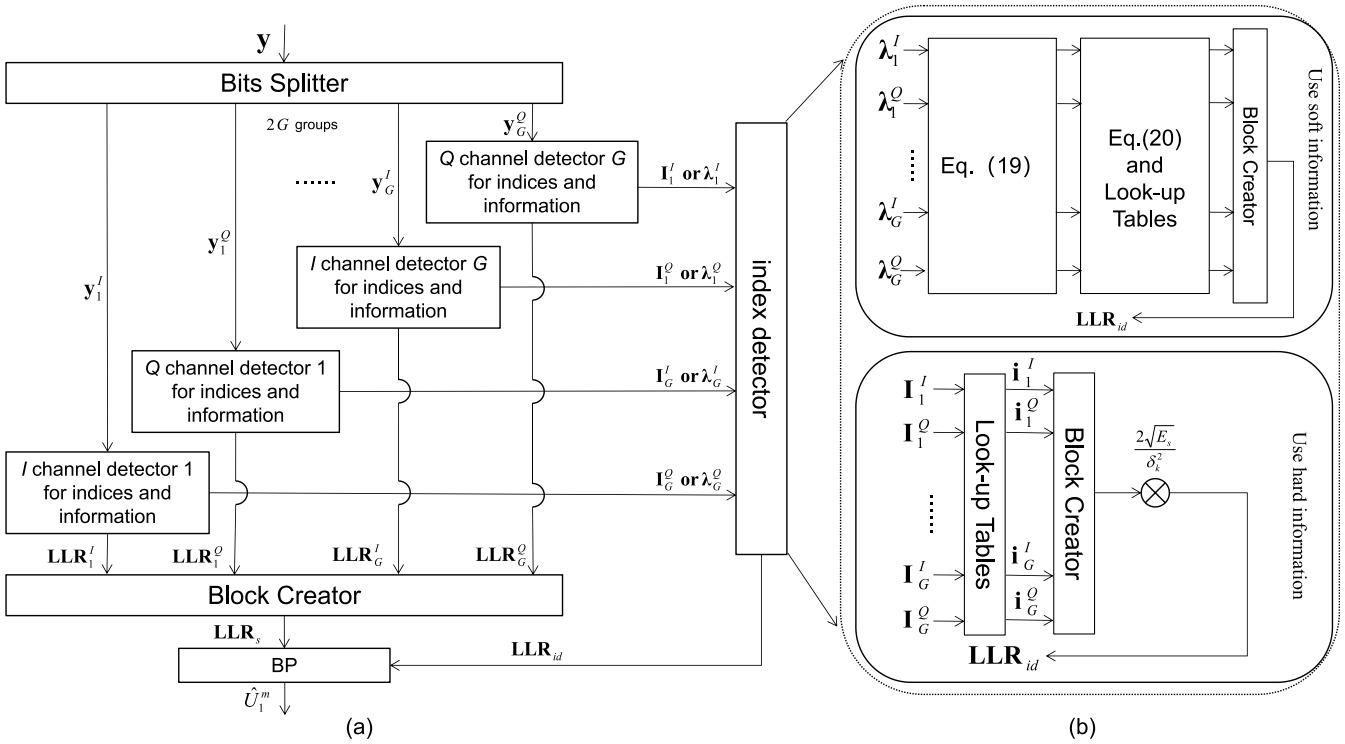

FIGURE 3. Block diagram of (a). a polar-coded OFDM-I/Q-IM receiver (b). an example of the initial LLR generation process of the indices bits using hard or soft information.

Here, we define a mapping according to the look-up tables:

$$i(j) = b \Leftrightarrow \mathbb{P}_{i(j)=b} \tag{18}$$

where $\mathbb{P}_{i(j)=b} = [\mathrm{P}_{b,1}, \ldots \mathrm{P}_{b,\omega} \ldots, \mathrm{P}_{b,V}]$ is the pattern corresponding to $i(j) = b$, where $b \in \{0, 1\}$. Pattern $\mathrm{P}_{b,\omega}$ is a length n sequence where the active position is denoted as $\times$ and the null position is denoted as 0. For example, according to Table.1, $\mathrm{P}_{0,1}$ and $\mathrm{P}_{0,2}$ can be written as: $[\times, 0, \times, 0]$ and $[0, \times, 0, \times]$, respectively. The probability that the η^{th} element in pattern $\mathrm{P}_{b,\omega}$ is zero or $\times$ can be written as:

$$\begin{aligned} P(\mathrm{P}_{b,\omega}(\eta) \text{ is } 0) &= \frac{1}{1+\exp(\lambda(\eta))} \\ P(\mathrm{P}_{b,\omega}(\eta) \text{ is } \times) &= \frac{\exp(\lambda(\eta))}{1+\exp(\lambda(\eta))} \end{aligned} \tag{19}$$

Then, the corresponding LLR of bit $i(j)$ can be written as:

$$LLR_{i(j)} = \ln\frac{P(i(j)=1|\mathbf{y})}{P(i(j)=0|\mathbf{y})} = \ln\frac{\sum_{\omega=1}^{V}\prod_{\eta=1}^{n} P(\mathrm{P}_{1,\omega}(\eta) \text{is } \mho_{i(j)=1})}{\sum_{\omega=1}^{V}\prod_{\eta=1}^{n} P(\mathrm{P}_{0,\omega}(\eta) \text{is } \mho_{i(j)=0})} \tag{20}$$

where $\mho \in \{\times, 0\}$, and $\mho_{i(j)=b}$ represents the active status of $\mathrm{P}_{b,\omega}$ corresponding to $i(j) = b$. The initial LLR calculation method using soft information is given in the upper part of Fig.3.(b).

For example, considering a sub-block with $n = 4$, $k = 2$, and Table.1, according to (19), the probability that $\mathrm{P}_{b,\omega}(\eta)$ with $b = \{0, 1\}$ equals to zero or not can be written as: $P(\mathrm{P}_{b,\omega}(\eta) \text{is} 0) = \frac{1}{1+\exp(\lambda(\eta))}$ and $P(\mathrm{P}_{b,\omega}(\eta) \text{is} \times) = \frac{\exp(\lambda(\eta))}{1+\exp(\lambda(\eta))}$ with $\eta = 1, 2, 3, 4$. Then, based on the mapping between $i(j)$ and $\mathbb{P}_{i(j)}$ with $1 \le j \le 2$. The probability that $i(1)$ equals to 0 or 1 can be written as ($i(2)$ can be obtained in a similar way):

$$\begin{aligned} P(i(1)=0|\mathbf{y}) = {} & P(\mathrm{P}_{0,1}(1) \text{ is } \times) \cdot P(\mathrm{P}_{0,1}(2) \text{ is } 0) \cdot \ldots \\ & \cdot P(\mathrm{P}_{0,1}(3) \text{ is } \times) \cdot P(\mathrm{P}_{0,1}(4) \text{ is } 0) \\ & + P(\mathrm{P}_{0,2}(1) \text{ is } 0) \cdot P(\mathrm{P}_{0,2}(2) \text{ is } \times) \cdot \ldots \\ & \cdot P(\mathrm{P}_{0,2}(3) \text{ is } 0) \cdot P(\mathrm{P}_{0,2}(4) \text{ is } \times) \\ P(i(1)=1|\mathbf{y}) = {} & P(\mathrm{P}_{1,1}(1) \text{ is } 0) \cdot P(\mathrm{P}_{1,1}(2) \text{ is } \times) \cdot \ldots \\ & \cdot P(\mathrm{P}_{1,1}(3) \text{ is } \times) \cdot P(\mathrm{P}_{1,1}(4) \text{ is } 0) \\ & + P(\mathrm{P}_{1,2}(1) \text{ is } \times) \cdot P(\mathrm{P}_{1,2}(2) \text{ is } 0) \cdot \ldots \\ & \cdot P(\mathrm{P}_{1,2}(3) \text{ is } 0) \cdot P(\mathrm{P}_{1,2}(4) \text{ is } \times) \end{aligned}$$

Then, according to (20), the corresponding LLR value of $i(1)$ can be obtained.

Compared with the LLR calculation method that using hard values, method that using soft information from $\lambda(\eta)$ fully takes advantage of the probabilities provided by channel detectors, which should bring benefit in terms of BER performance. However, this method owns higher complexity, especially when $\mathbb{C}_n^k$ is large. The computational complexity of the soft information based method can be roughly generalized to $O(2^{\lfloor \log_2 \mathbb{C}_n^k \rfloor})$ per sub-carrier and dimension. The simulation result (Fig.5) show that although using (19) and (20) to generate initial LLRs can achieve better performance, using (17) can still obtain a good performance with lower complexity.

After obtaining the LLRs of index bits, which are denoted as $\mathbf{LLR}_{id}$, LLRs of the rest transmitted codewords need

TABLE 5. Simulation parameters.

Number of available subcarriers (N_{fft})	64
Modulation	4-QAM
Length of cyclic prefix	8
Length of polar code (N)	128
Number of information bits (m)	$\{64, 84\}$
Number of indices bits (b_1)	$\{2, 4\}$
Number of sub-blocks (G)	$\{8, 16\}$

to be confirmed. First, for the g^{th} sub-block, we write the symbols after idle sub-carriers removal as:

$$\{S_g(\eta)\}_{\eta=1}^{k} = [S_g(1), S_g(2), \ldots, S_g(k)] \tag{21}$$

Each symbol $S_g(\eta)$ consists $\log_2 M$ bits. Denote $Q_{c,i}$ as the sub-constellation of Q corresponding to bit c among $\log_2 M$ bits when bit c is $i \in \{0, 1\}$. Then, for a given $S_g(\eta)$, the LLR of bit c is given by:

$$\begin{aligned} LLR_{g,c}(\eta) &= \ln \frac{P(y_g(\eta)|\langle S_g(\eta)\rangle_c = 0)}{P(y_g(\eta)|\langle S_g(\eta)\rangle_c = 1)} \\ &= \ln \frac{\sum_{S\in Q_{c,0}} \exp(-\frac{|y_g(\eta)-H_g(\eta)S|^2}{\sigma_k^2})}{\sum_{S\in Q_{c,1}} \exp(-\frac{|y_g(\eta)-H_g(\eta)S|^2}{\sigma_k^2})} \end{aligned} \tag{22}$$

where $\langle S(\eta)\rangle_c$ denotes the c^{th} bit of the symbol S. Then, combining with the $\mathbf{LLR}_{id}$, the N length LLRs becomes the initial input of the polar decoding part to obtain the estimated information bits $\hat{U}_1^m$. In this paper, a widely used BP decoding scheme [26], which is a type of soft input and soft output (SISO) decoding, is applied in both the proposed system and the polar-coded OFDM system for fair comparison. Also, we note that the successive cancellation (SC) based decoding can be used in the proposed system.

IV. SIMULATION RESULTS AND EVALUATION

In this section, methods proposed in above sections are verified, and the BER performance of the proposed polar-coded OFDM-I/Q-IM system is investigated. To make fair comparisons, both the proposed polar-coded OFDM-I/Q-IM and polar-coded OFDM are compared with the same transmission rate R, where $R = m/N_{fft}$. Perfect channel estimation was assumed. The parameters used in simulations are given in Table.5.

Fig.4 gives the BER performance between the polar-coded OFDM-I/Q-IM systems using different bits appending methods. The number of sub-block G is 8. When $b_1 = 2$, each sub-block has $n = 8$ available sub-carriers, and $k = 6$ sub-carriers are activated. Hence, $p_1 - b_1 = 2$ extra bits are appended. By appending random frozen bits, the corresponding BER performance can be improved. Therefore, we note that in the following simulations, the proposed appending method is applied whenever $p_1 > b_1$.

Then, BER performances of the proposed systems utilizing different LLRs calculation methods in Fig.3.(b). are investigated. Fig.5 illustrates that compared with the initial LLRs obtained from (20), using the initial LLRs obtained through hard information caused BER degradation. In low-mid SNR, the gap is negligible. Nevertheless, the gap becomes larger

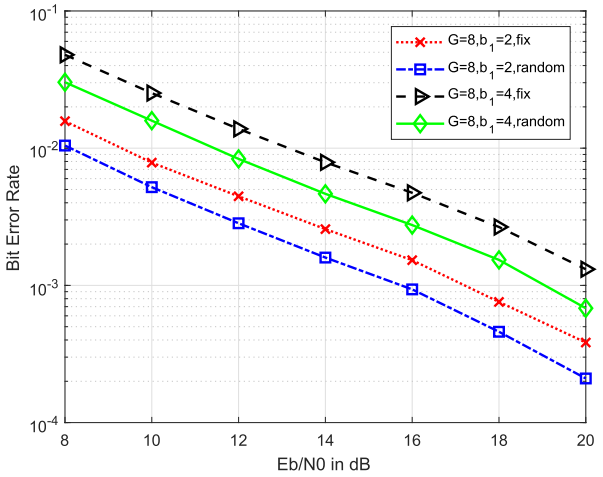

FIGURE 4. BER performance between the polar-coded OFDM-I/Q-IM systems using different appending methods.

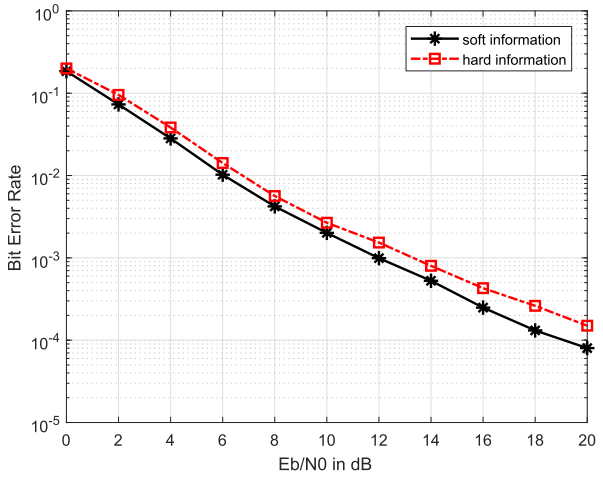

FIGURE 5. BER performance between different LLR generation methods.

in high SNR scenarios. At probability 1.6×10^{-4}, the black line which soft information are applied has around 2 dB performance gain compared with the red line that hard values are utilized. However, in terms of computational complexity, using hard valued sequence is an effective way to implement the decoding procedure. Therefore, in the following simulations, the LLRs calculation method using hard-valued sequences is utilized for simplicity.

The BER comparison between the proposed polar-coded OFDM-I/Q-IM system (denoted as "proposed") and the conventional polar-coded OFDM system (denoted as "P-OFDM") with different transmission rate R is given in Fig.6. As a reference, the performance of a pure OFDM-I/Q-IM [10] and a polar-coded OFDM in slow Rayleigh fading channel (denoted as "O-PC-Frequency non selective") [14] are also included. In the simulation, $G = 16$, $b_1 = 4$. It was illustrated that compared with the OFDM-I/Q-IM, adding polar codes was helpful in terms of BER performance. Then, the proposed system can achieve significant BER enhancement compared with the conventional polar-coded OFDM. For example, when $R = 1$, at probability 10^{-3},

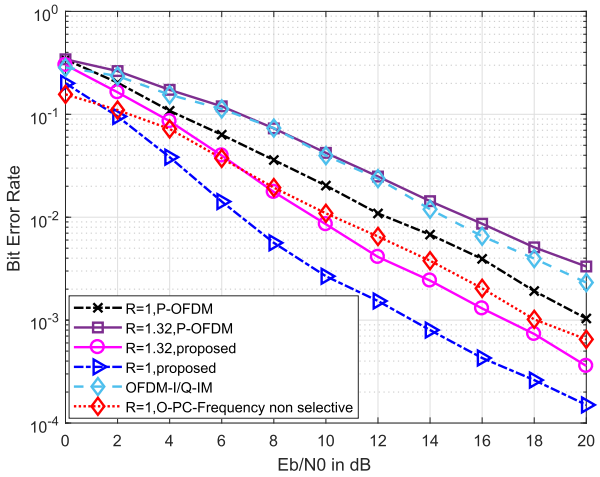

FIGURE 6. BER performance between the proposed system and polar-coded OFDM.

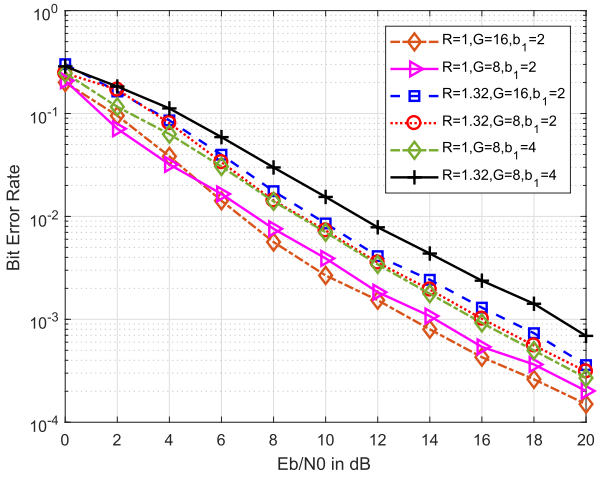

FIGURE 7. BER performance of the proposed systems with various G and b_1.

the proposed system obtained around 6 dB gains than that of the conventional polar-coded OFDM system.

Then, BER performance of the proposed polar-coded OFDM-I/Q-IM system by utilizing different number of sub-block G and index bits b_1 is investigated. Fig.7 indicates that various G and b_1 can cause different BER performances. When $G = 8$, and $b_1 = 4$, no matter what transmission rate R is, the corresponding BER performance is the worst compared with other allocation ways due to its large SAPs [27]. Intuitively, it was expected that when b_1 is same, larger G would bring better performance because more index bits can be used for decoding. However, it is shown that in some cases, the allocation method using $G = 8$, $b_1 = 2$ achieves better BER performance than that of the method using $G = 16$, $b_1 = 2$ (The red and blue solid lines when $R = 1.32$). It can be explained by the index error rate (IER). We provide the corresponding IER result among different index allocations in Fig.8. It is illustrated that although the scheme using $G = 16$, $b_1 = 2$ has more index bits sent to the BP decoder, it also causes higher IER. Therefore, it is possible for the scheme using $G = 8$, $b_1 = 2$ to achieve better overall BER performance.

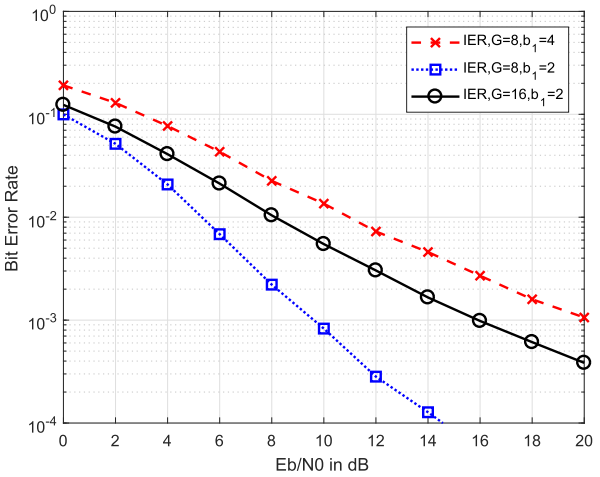

FIGURE 8. IER performance of the proposed systems with different index bits allocations.

V. CONCLUSION

In this paper, a polar-coded OFDM-IM system is proposed. By introducing the concept of index modulation, the polar codeword can be transmitted not only by OFDM blocks, but also indices of active sub-carriers. For the proposed system, a part of polar codewords are transmitted implicitly through index modulation. Unlike the polar-coded OFDM, using polar codes in OFDM-IM systems has difficulties in terms of bits allocations due to the length and constellation restrictions of polar codes. Therefore, OFDM-I/Q-IM and random frozen bits appending method are introduced and proposed to make polar codes more compatible for OFDM-IM based systems. At the receiver, the index detector and a BP decoder are utilized for data recovery. For the proposed system, the detected index bits are regarded as reliable and the corresponding initial LLRs for decoding can be obtained through soft or hard information provided by such index detector. These initial LLRs are helpful to achieve better decoding performance. Simulation results show that the proposed polar-coded OFDM-I/Q-IM system can achieve significantly better BER performance than that of the conventional polar-coded OFDM system with different transmission rate. Nevertheless, how to obtain the initial LLRs of index bits with low complexity is still open for future research.

APPENDIX

Here, we prove the conclusion claimed in the previous section that the IER of OFDM-I/Q-IM is lower than the BER of M-QAM demodulation. Let take an OFDM-I/Q-IM scheme with parameters n and k as an example. On the one hand, it is known that the estimation procedure of the activity of a single sub-carrier is similar to coherent binary ASK detection which probability of error over Rayleigh fading channels can be given as [28]:

$$P_{BASK} = 0.5(1 - \sqrt{\frac{\gamma_b}{1+\gamma_b}}) \tag{23}$$

where $\gamma_b = \alpha^2 \frac{E_b}{N_0}$ is the average SNR per bit, α is the average fading amplitude and E_b is the average bit energy. To have d errors, for a given n and k, the number of different sub-carrier

states between a transmitted SAP_i and incorrectly received SAP_j is given as [27]:

$$d_{i,j} = \sum_{\mu=1}^{n} (\text{SAP}_{i,\mu} \oplus \text{SAP}_{j,\mu}) \tag{24}$$

where $1 \leq i \leq 2^{p_1}$, $1 \leq j \neq i \leq \mathbb{C}_n^k$, μ is denoted as an inactivated sub-carrier index and $\oplus$ is an exclusive NOR operator. Hence, the probability of incorrectly detecting an SAP with $d_{i,j}$ sub-carrier detection errors is:

$$P_{ICi,j} = P_{BASK}^{d_{i,j}} \tag{25}$$

The average probability of incorrectly detecting SAPs can be written as:

$$P_{IC} = \frac{1}{2^{p_1}(\mathbb{C}_k^n - 1)} \sum_{i=1}^{2^{p_1}} \sum_{j=1, j\neq i}^{\mathbb{C}_k^n} P_{ICi,j} \tag{26}$$

Considering an incorrect SAP, it is shown in [29] that an incorrect detected SAP causes an average error of about $0.5p_1$ in the de-mapped p_1 bits. Hence, the IER contribution of an incorrect detected SAP is:

$$B_{IC} = P_{IC}(\frac{0.5p_1}{p_1}) = 0.5P_{IC} \tag{27}$$

On the other hand, the approximate BER P_b of M-QAM demodulation over Rayleigh fading channels can be written as [30]:

$$\begin{aligned} P_b = {} & \frac{2}{\log_2 M}(\frac{\sqrt{M}-1}{\sqrt{M}}) \\ & \times (1 - \sqrt{\frac{1.5\gamma_s}{M-1+1.5\gamma_s}}) - (\frac{\sqrt{M}-1}{\sqrt{M}})^2 \\ & \times \frac{1}{\log_2 M}[1 - \sqrt{\frac{1.5\gamma_s}{M-1+1.5\gamma_s}}) \\ & \times (\frac{4}{\pi}\tan^{-1}\sqrt{\frac{1.5\gamma_s}{M-1+1.5\gamma_s}})] \end{aligned} \tag{28}$$

where $\gamma_s = \gamma_b \log_2 M$ is the average SNR per symbol.

To prove the IER for the OFDM-I/Q-IM scheme is lower than the BER of the conventional M-QAM demodulation ($B_{IC} < P_b$), let assume $M = 4$, $n = 4$, and $k = 2$ (using Table.1). It is illustrated that when using Table.1, the errors d in a received SAP is larger than 2, given as:

$$d_{i,j} = \sum_{\mu=1}^{n} (\text{SAP}_{i,\mu} \oplus \text{SAP}_{j,\mu}) \geqslant 2$$

Thus $P_{IC,i,j} \leq P_{BASK}^2$. Then, the B_{IC} in (27) can be rewritten as:

$$\begin{aligned} B_{IC} &= 0.5P_{IC} \\ &= \frac{0.5}{2^{p_1}(\mathbb{C}_k^n - 1)} \sum_{i=1}^{2^{p_1}} \sum_{j=1, j\neq i}^{\mathbb{C}_k^n} P_{ICi,j} \\ &\leq 0.5 \times 1 \times P_{BASK}^2 \\ &\leq 0.5P_{BASK}^2 \end{aligned} \tag{29}$$

Then, for the conventional 4-QAM demodulation, the corresponding P_b can be denoted as:

$$\begin{aligned} P_b &\geq \frac{1}{2}(1 - \sqrt{\frac{\gamma_b}{1+\gamma_b}}) - \frac{1}{8}(1 - \sqrt{\frac{\gamma_b}{1+\gamma_b}} \times \frac{4}{\pi} \times \frac{\pi}{4}) \\ &\geq P_{BASK} - \frac{1}{4}P_{BASK} \\ &\geq \frac{3}{4}P_{BASK} \end{aligned} \tag{30}$$

Therefore: $B_{IC} - P_b \leq \frac{1}{2}P_{BASK}^2 - \frac{3}{4}P_{BASK} < 0$. Thus the bits detected by indices detector is more reliable and may benefit the decoding procedure.

REFERENCES

[1] E. Arikan, "Channel polarization: A method for constructing capacity-achieving codes for symmetric binary-input memoryless channels," *IEEE Trans. Inf. Theory*, vol. 55, no. 7, pp. 3051–3073, Jul. 2009.
[2] K. Niu, K. Chen, J. Lin, and Q. Zhang, "Polar codes: Primary concepts and practical decoding algorithms," *IEEE Commun. Mag.*, vol. 52, no. 7, pp. 192–203, Jul. 2014.
[3] K. Niu and K. Chen, "CRC-aided decoding of polar codes," *IEEE Commun. Lett.*, vol. 16, no. 10, pp. 1668–1671, Oct. 2012.
[4] V. Bioglio, C. Condo, and I. Land, "Design of polar codes in 5G new radio," *IEEE Commun. Surveys Tuts.*, early access, Jan. 17, 2020, doi: 10.1109/COMST.2020.2967127.
[5] E. Başar, Ü. Aygölü, E. Panayırı, and H. V. Poor, "Orthogonal frequency division multiplexing with index modulation," *IEEE Trans. Signal Process.*, vol. 61, no. 22, pp. 5536–5549, Aug. 2013.
[6] E. Basar, "Index modulation techniques for 5G wireless networks," *IEEE Commun. Mag.*, vol. 54, no. 7, pp. 168–175, Jul. 2016.
[7] M. Wen, B. Zheng, K. J. Kim, M. Di Renzo, T. A. Tsiftsis, K.-C. Chen, and N. Al-Dhahir, "A survey on spatial modulation in emerging wireless systems: Research progresses and applications," *IEEE J. Sel. Areas Commun.*, vol. 37, no. 9, pp. 1949–1972, Sep. 2019.
[8] E. Basar, "OFDM with index modulation using coordinate interleaving," *IEEE Wireless Commun. Lett.*, vol. 4, no. 4, pp. 381–384, Aug. 2015.
[9] E. Basar, "Index modulation: A promising technique for 5G and beyond wireless networks," in *Networks of the Future: Architectures, Technologies, and Implementations*, 1st ed. London, U.K.: Chapman & Hall, 2017. [Online]. Available: https://corelab.ku.edu.tr/wp-content/uploads/2018/07/Index-Modulation-A-Promising-Technique-for-5G-and-Beyond-Wireless-Networks.pdf
[10] R. Fan, Y. J. Yu, and Y. L. Guan, "Generalization of orthogonal frequency division multiplexing with index modulation," *IEEE Trans. Wireless Commun.*, vol. 14, no. 10, pp. 5350–5359, Oct. 2015.
[11] Y. Xiao, S. Wang, L. Dan, X. Lei, P. Yang, and W. Xiang, "OFDM with interleaved subcarrier-index modulation," *IEEE Commun. Lett.*, vol. 18, no. 8, pp. 1447–1450, Aug. 2014.
[12] J. Choi, "Coded OFDM-IM with transmit diversity," *IEEE Trans. Commun.*, vol. 65, no. 7, pp. 3164–3171, Jul. 2017.
[13] B. Zheng, F. Chen, M. Wen, F. Ji, H. Yu, and Y. Liu, "Low-complexity ML detector and performance analysis for OFDM with in-phase/quadrature index modulation," *IEEE Commun. Lett.*, vol. 19, no. 11, pp. 1893–1896, Nov. 2015.
[14] R. Umar, F. Yang, S. Mughal, and H. Xu, "Distributed polar-coded OFDM based on Plotkin's construction for half duplex wireless communication," *Int. J. Electron.*, vol. 105, no. 7, pp. 1097–1116, Jul. 2018.
[15] D. R. Wasserman, A. U. Ahmed, and D. W. Chi, "BER performance of polar coded OFDM in multipath fading," 2016, *arXiv:1610.00057*. [Online]. Available: http://arxiv.org/abs/1610.00057
[16] M. Wen, Q. Li, E. Basar, and W. Zhang, "Generalized multiple-mode OFDM with index modulation," *IEEE Trans. Wireless Commun.*, vol. 17, no. 10, pp. 6531–6543, Oct. 2018.
[17] M. Wen, B. Ye, E. Basar, Q. Li, and F. Ji, "Enhanced orthogonal frequency division multiplexing with index modulation," *IEEE Trans. Wireless Commun.*, vol. 16, no. 7, pp. 4786–4801, Jul. 2017.
[18] J. Li, S. Dang, M. Wen, X.-Q. Jiang, Y. Peng, and H. Hai, "Layered orthogonal frequency division multiplexing with index modulation," *IEEE Syst. J.*, vol. 13, no. 4, pp. 3793–3802, Dec. 2019.

[19] D. Wu, Y. Li, and Y. Sun, "Construction and block error rate analysis of polar codes over AWGN channel based on Gaussian approximation," *IEEE Commun. Lett.*, vol. 18, no. 7, pp. 1099–1102, Jul. 2014.
[20] R. Wang, J. Honda, H. Yamamoto, R. Liu, and Y. Hou, "Construction of polar codes for channels with memory," in *Proc. IEEE Inf. Theory Workshop Fall (ITW)*, Oct. 2015, pp. 187–191.
[21] E. Sasoglu and I. Tal, "Polar coding for processes with memory," *IEEE Trans. Inf. Theory*, vol. 65, no. 4, pp. 1994–2003, Apr. 2019.
[22] N. Ishikawa, S. Sugiura, and L. Hanzo, "Subcarrier-index modulation aided OFDM–Will it work?" *IEEE Access*, vol. 4, pp. 2580–2593, 2016.
[23] V. Miloslavskaya, "Shortened polar codes," *IEEE Trans. Inf. Theory*, vol. 61, no. 9, pp. 4852–4865, Sep. 2015.
[24] R. Wang and R. Liu, "A novel puncturing scheme for polar codes," *IEEE Commun. Lett.*, vol. 18, no. 12, pp. 2081–2084, Dec. 2014.
[25] P. Robertson, E. Villebrun, and P. Hoeher, "A comparison of optimal and sub-optimal MAP decoding algorithms operating in the log domain," in *Proc. IEEE Int. Conf. Commun. (ICC)*, vol. 2, Jun. 1995, pp. 1009–1013.
[26] B. Yuan and K. K. Parhi, "Architecture optimizations for BP polar decoders," in *Proc. IEEE Int. Conf. Acoust., Speech Signal Process.*, May 2013, pp. 2654–2658.
[27] A. I. Siddiq, "Effect of subcarrier activation ratio on the performance of OFDM-IM over Rayleigh fading channel," *IEEE Commun. Lett.*, vol. 21, no. 6, pp. 1293–1296, Jun. 2017.
[28] M.-S. Alouini and A. J. Goldsmith, "A unified approach for calculating error rates of linearly modulated signals over generalized fading channels," *IEEE Trans. Commun.*, vol. 47, no. 9, pp. 1324–1334, 1999.
[29] A. Ikram Siddiq, "Low complexity OFDM-IM detector by encoding all possible subcarrier activation patterns," *IEEE Commun. Lett.*, vol. 20, no. 3, pp. 446–449, Mar. 2016.
[30] R. Abu-alhiga and H. Haas, "Subcarrier-index modulation OFDM," in *Proc. IEEE 20th Int. Symp. Pers., Indoor Mobile Radio Commun.*, Sep. 2009, pp. 177–181.

SI-YU ZHANG (Graduate Student Member, IEEE) received the B.A.Sc. degree from Jilin University, China, in 2014, and the M.A.Sc. degree in electrical engineering from the University of Windsor, Ontario, Canada, in 2016, where he is currently pursuing the Ph.D. degree. His current research interests include PAPR reduction techniques, OFDM and OFDM-IM systems, coding, and information theory, especially the design of polar decoders for 5G wireless networks.

BEHNAM SHAHRRAVA (Member, IEEE) received the Ph.D. degree in electrical engineering from the University of Waterloo, Ontario, Canada, in 1998. He is currently an Associate Professor with the Department of Electrical and Computer Engineering, University of Windsor, Ontario, Canada. His research interests are in the areas of advanced statistical and adaptive signal processing and their applications, primarily in wireless communications, multiuser detection, iterative decoding algorithms, and turbo receiver design.